Supplementary Information for "Soft Conductive Hydrogel Micropillar For Electrophysiological Recording"

Yuxin Liu[1†], Allister F. McGuire[2†], Hsin-Ya Lou[2], Thomas L. Li[2], Jeffrey B.-H. Tok[3], Bianxiao Cui[2]*, Zhenan Bao[3]*

[1]Department of Bioengineering, Stanford University, Stanford, California 94305, USA

[2]Department of Chemistry, Stanford University, Stanford, CA 94305, USA

[3]Department of Chemical Engineering, Stanford University, Stanford, California 94305, USA

* Corresponding author. E-mail: zbao@stanford.edu; bcui@stanford.edu

† These authors contributed equally to this work.

www.pnas.org/cgi/doi/10.1073/pnas.1810827115

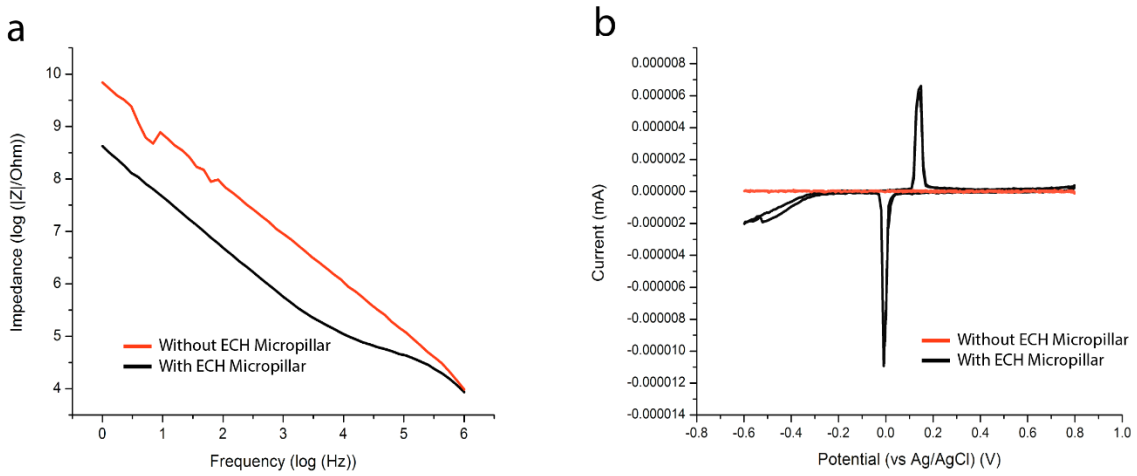

Figure S1. Impedance spectra over frequency (a) and cyclic voltammetry (scan rate at 50mV/s) (b) comparison for three-dimensional ECH micropillar on Pt electrode (Black line; with ECH micropillar) and planar Pt electrode (Red line; without ECH micropillar).

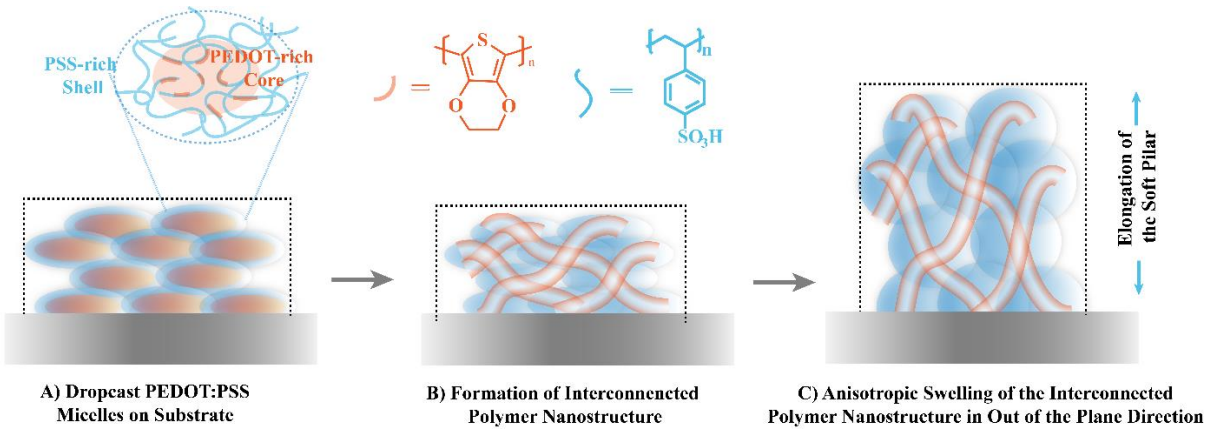

Figure S2. Proposed schematic illustration of the anisotropic swelling of PEDOT:PSS. (A) The PEDOT:PSS micelles, which have a PSS-rich shell and PEDOT-rich core, are drop cast onto the substrate. During the water evaporation process in drop casting, the PEDOT:PSS micelles are deformed by thickness reduction in the out of the plane direction, forming a "pancake"-like morphology (B) Interconnected nanostructure is induced in the polymer by ionic liquid 4-(3-Butyl-1-imidazolio)-1-butanesulfonic acid triflate. (C) Anisotropic swelling occurs in the out of the plane direction. The interconnected polymer nanostructure prevents dissolution of micropillar.

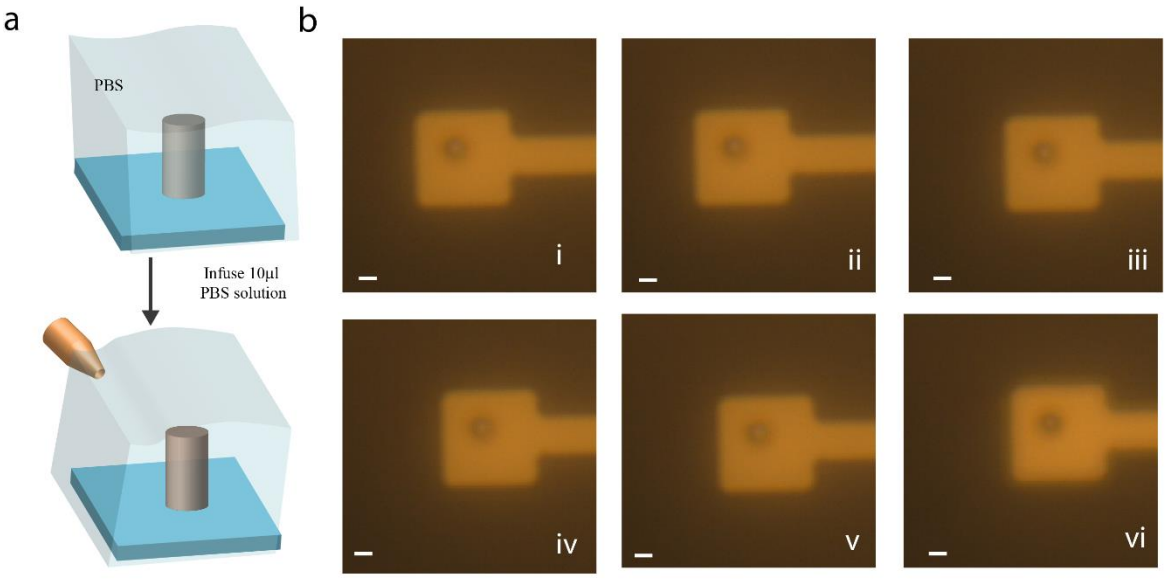

Figure S3. (a) Schematic illustration of the mechanical perturbation experiment injecting 10 µl PBS solution towards the IrOx micropillar. (b) Optical microscope image of an IrOx micropillar when 10 µl of PBS solution is injected at various times. 0 s (i), 2 s (ii), 4 s (iii), 6 s (iv), 8 s (v), 10 s (vi). There is no measurable rotation or bending of IrOx micropillar observed. Scale bars: 5 µm.

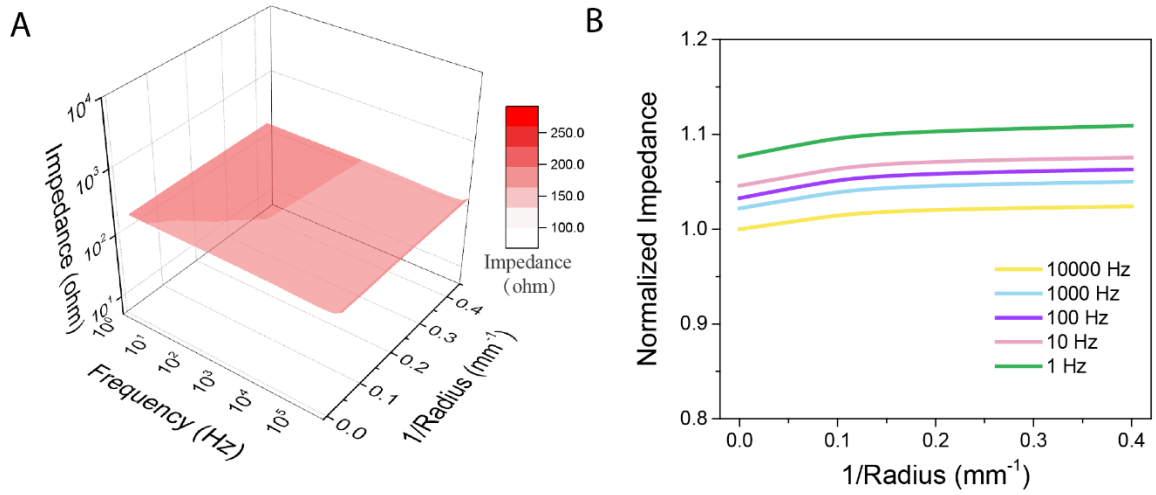

Figure S4. Electrochemical impedance of the pillar during bending. (A) Surface plot of electrochemical impedance at various frequencies and bending curvature. The ECH pillar (cross sectional area: 1 mm^2; height: 4.3 mm) was bent in PBS solution during electrochemical impedance measurement. (B) Normalized impedance of the pillar at various bending radii for frequency at 1 Hz, 10 Hz, 100 Hz, 1 kHz and 10 kHz.

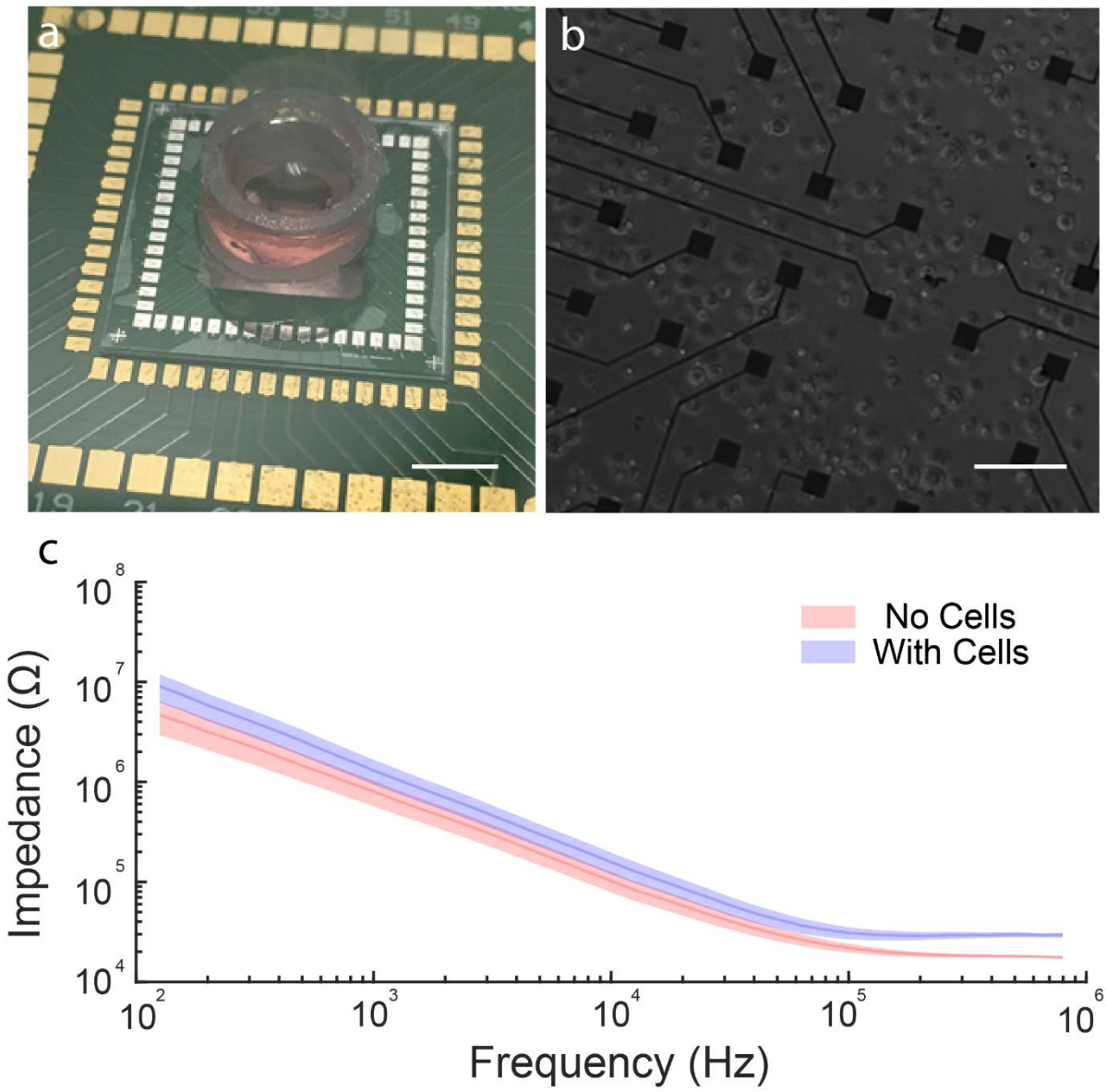

Figure S5 (a) Photo of soft multielectrode array (S-MEA) with cell culture media and HL-1 cells. (b) Inverted microscope image of HL-1 seeded on the ECH MEA. (c) Impedance spectra of the same electrode before and after seeding of HL-1 cells. The increased impedance suggests the formation of tight sealing at cell-electrode interface. Shaded area denotes s.d., N = 60.

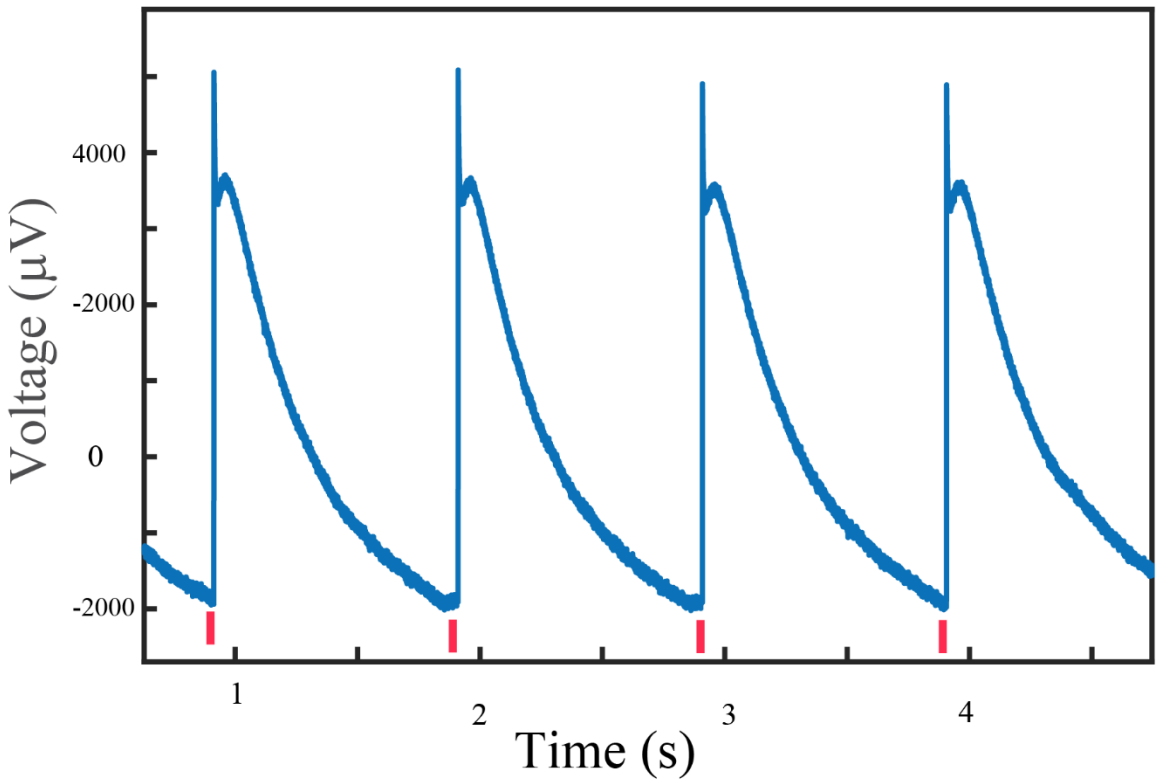

Figure S6. Extracellular recording with ECH micropillars for HL-1 cells paced at 1 Hz (paced voltage of 1 V, 200 μs square wave pulse). Red bar: pulse of electrical stimulation

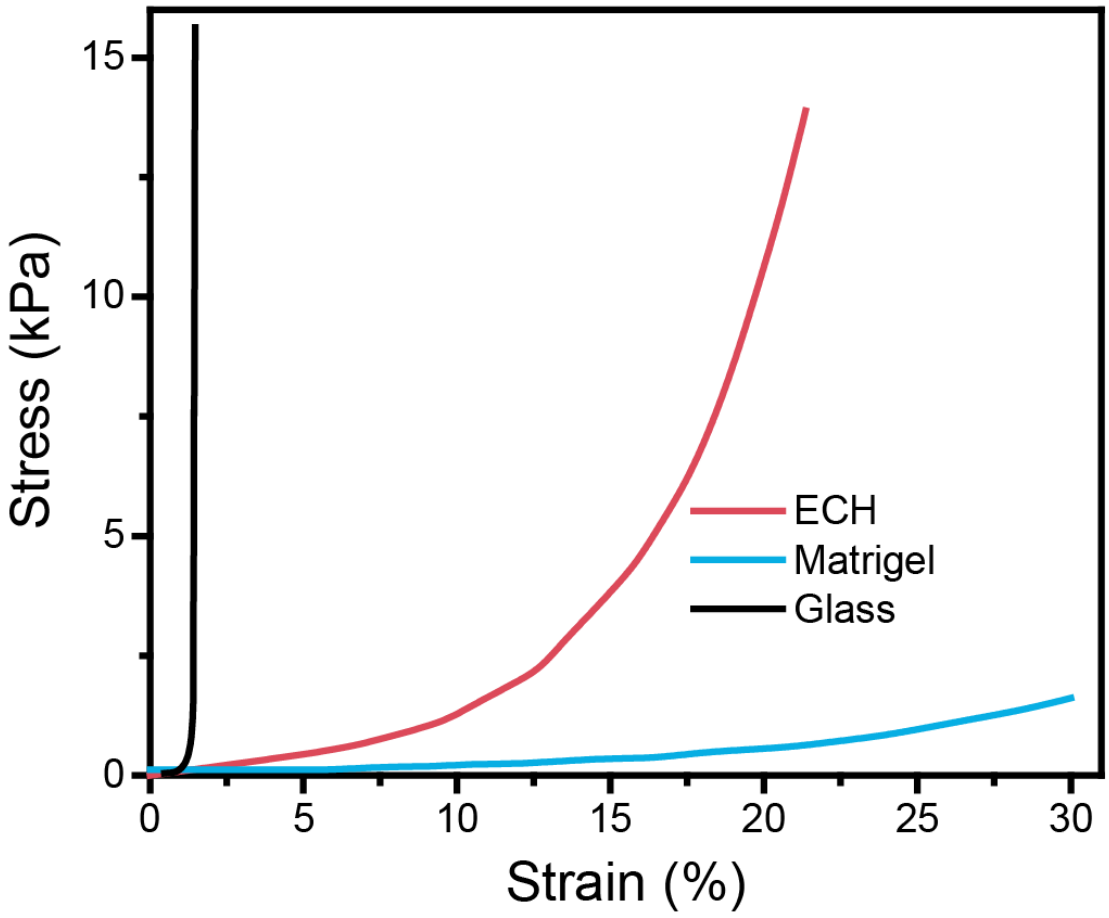

Figure S7. Stress-strain curve of ECH (6 mm × 6 mm with thickness of 0.05 mm) compared to a stiff substrate, glass (5 mm × 8.7 mm with thickness of 0.9 mm), and Matrigel (a gelatinous protein mixture used as extracellular matrix for cell culture; 5.3 mm × 86.3 mm with thickness of 0.05 mm).